A Comparative Study of Cation and Anion Cluster Reaction Products: The Reaction Mechanisms of Lead Clusters with Benzene in Gas Phase

Xiaopeng Xing, Zhixin Tian, Hongtao Liu, and Zichao Tang*

State Key Laboratory of Molecular Reaction Dynamics, Center of Molecular Science, Institute of Chemistry, Chinese Academy of Sciences, Beijing 100080, P. R. China

Received: April 27, 2003; In Final Form: July 18, 2003

The cation and anion products of the reactions between lead clusters produced in the laser ablation and the benzene molecules seeded in argon were studied by high-resolution reflectron time-of-flight mass spectrometer (RTOFMS). The dominant cation products were Pb/benzene association complexes, while the dominant anion products were dehydrogenated species, $[Pb_mC_n]^-$, $[Pb_mC_nH_k]^-$, etc. One important intermediate distinguished in the anion reactions was $[Pb_m(C_6H_5)]^-$ product. Two conspicuously different and independent reaction mechanisms were proposed for lead cluster cations and anions, respectively.

Introduction

Studies on the chemical interactions between metal clusters and organic molecules can provide useful information, which leads to deep understanding of some important heterogeneous catalytic processes in the organometallic chemistry field. As a fundamental chemical issue in theoretical study and industry application, the adsorption and dissociation of benzene on the metal cluster surfaces have been hot topics for many years.[1−6] The structure and property of metal−aromatic molecular complexes have been studied extensively.

The advents of the laser vaporization and the molecular beam techniques have promoted a rapid progress in these studies. Duncan and co-workers[7,8] have investigated the dissociation processes of metal cation−benzene complexes in gas phase and discussed the dissociative charge-transfer progress in detail. Koji Kaya and co-workers[9−11] have synthesized neutral 3d transition metal−benzene complexes through the reactions between metal clusters and benzene in gas phase. They studied the mass distribution, the reactivity, and the ionization energy of these complexes and presented two different structures: (1) sandwich structure (for Sc, Ti, V, etc.) in which the metal atom was separated by benzene molecules one by one and (2) rice-ball structure (for Fe, Co, Ni, etc.) in which the metal clusters were surrounded by benzene molecules.

However, these studies focused mainly on the transition metal species, and much work is still required on the reactions of the main group metals. Lead has a completely different electronic structure from those of the transition metals, and many unfilled orbitals (for example, those in Pb_2^+) or unpaired electrons (for example, those in Pb_m^-) are present in lead clusters. This may exert influence on their reactions or bonds with benzene. In industry, lead is involved in some important catalytic processes. Lead ruthenate has catalytic activity comparable with that of Pt in the catalytic decomposition of hydrogen peroxide in alkaline solution.[12] Lead halides are used to catalyze the allylation of biphenyl ether with allyl bromide and give good functional selectivity.[13] In addition to its practical application, the study of lead cluster ions is also of fundamental interest. As early as 1972, Castleman and co-workers[14] studied the gas-phase hydration of the monovalent lead cation using high-pressure mass spectrometry, and clusters of up to eight water molecules around a lead cation were observed. Later, the same group reported the combination reaction of benzene with lead cation.[15] Very recently, A. J. Stace and co-workers[16] found that lead cluster cations combined with methanol molecules to form lead/methanol complexes and the lead moiety can catalyze the bimolecular dehydration through the O−H insertion. In our previous works,[17,18] we have shown that in the reactions between lead cluster ions and alkene or acetone, they could insert into the C−C or C−H bond through high-energy reaction pathway.

In this paper, the reactions between lead cluster ions and benzene molecules were performed on one laser ablation and buffer gas ion source. The products were analyzed using a high-resolution reflectron time-of-flight mass spectrometer (RTOFMS). Different reaction processes and bonding patterns were observed for the lead cluster cations and anions. The mechanisms involved in these reactions were discussed in detail.

Experimental Section

The apparatus consisted of a Smalley-type[19] laser vaporization source and a homemade high-resolution reflectron time-of-flight mass spectrometer (similar to that of Mamyrin[20]). A detailed description of the apparatus has been given elsewhere,[18,21] and only an outline was given here.

In the experiment, the lead sample was mounted 10 mm downstream from the nozzle (General Valve series 73, orifice diameter 0.8 mm) in the source chamber and ablated by the focused second harmonic output of a Nd:YAG laser (10 mJ/pulse, 10 Hz, 1 mm in diameter of beam spot). The metal particles were vaporized into the tube reactors (Ø3 × 10 mm), where high-pressure argon and small proportion of benzene were present. The clustering processes and the reactions with benzene were completed near the nozzle exit.[22] The products were cooled by supersonic expansion into vacuum through a 0.75 mm diameter orifice opening into a 5° (half-angle) conical nozzle. The expansion beam was skimmed by a conical skimmer (throat diameter of 2.5 mm) positioned about 30 mm downstream from the former nozzle and then entered the accelerator region of the RTOFMS.

* Corresponding author. Fax: +86-10-62563167. E-mail: zichao@mrdlab.icas.ac.cn.

10.1021/jp0351369 CCC: $25.00
Published on Web 09/12/2003

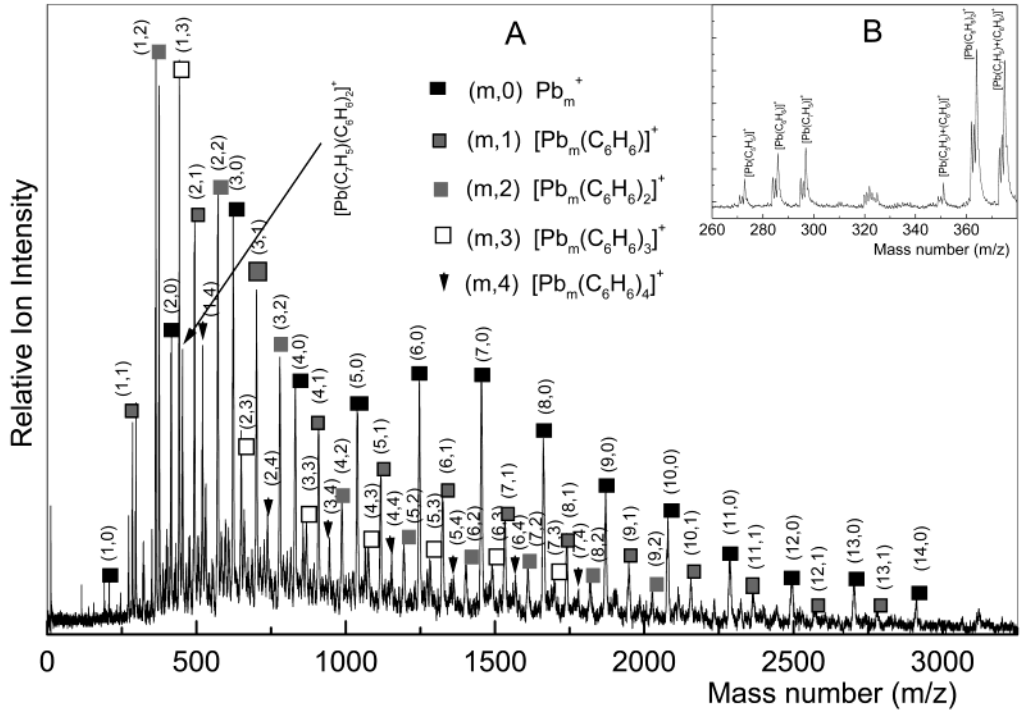

Figure 1. Typical mass spectra of the cation products by laser ablation of lead into the mixed gas of argon and benzene (2.5% benzene in 400 kPa mixed gas). The inset (panel B) showed the enlarged mass field of the fragment species ($[Pb(C_5H_5)]^+$, $[Pb(C_7H_5)]^+$, $[Pb(C_5H_5)(C_6H_6)]^+$, and $[Pb(C_7H_5)(C_6H_6)]^+$).

The pulsed electric field was operated in two polarity modes to detect either cationic or anionic products. In addition, one positive direct electric field combined with another ionization laser (Lambda Physik, Compex 103, 193 nm) in the accelerator region was used for neutral species detection. The products were then extracted and accelerated to about 1.2 keV perpendicularly. They experienced two sets of deflectors and electrostatic einzel lenses and then were reflected by a reflector. Finally the ions reached a dual microchannel plate (MCP). The output signal from the MCP was amplified and recorded by a 100 MHz transient recorder (USTC, China) and then was stored by a PC computer. The time sequence of valve opening, laser vaporization, pulse acceleration, and recording was optimized by a digital delay pulse generator (Stanford Research DG535). Typically the final digitized mass spectra were averaged 300 pulses, and the mass resolution of the mass spectrometer ($m/\Delta m$) could reach 2000. This enabled the apparatus to resolve the number of the hydrogen atoms coexisting in products easily.

The source chamber, the flight tube, and the reflectron region were all differentially pumped with mechanical pumps and turbomolecular pumps. The corresponding operating pressures were 10^{-4}, 10^{-6}, and 10^{-7} Torr, respectively.

The lead target was prepared by pressing lead powder (purity 99%) into a tablet, which was 12 mm in diameter and 5 mm in thickness. The benzene (analytical reagent) was seeded in argon (purity 99.9%) within a vacuum stainless steel bottle (about 1 L) to yield a total stagnation pressure of 400 kPa; the partial pressure of benzene was lower than 10 kPa (about 2.5% of the mixed gas). All materials and chemical reagents were obtained commercially and used as supplied without any further purification.

Results and Discussion

3.1. Reactions between Lead Cluster Cations and Benzene. The reactions between lead cluster cations and different concentration benzene in argon gas were investigated. Figure 1 showed a typical mass spectrum of the products when the benzene concentration was 2.5% of the mixed gas.

3.1.1. Pb/Benzene Association Cation Products. Pb_m^+ series were among the strongest cationic species in Figure 1, and a wide distribution ($m = 1-14$) was observed. The "magic numbers" of lead clusters, Pb_7^+, Pb_{10}^+, etc., observed elsewhere[23] were not apparent in this experiment. Their dominant reaction channel was association of benzene, forming $[Pb_m(\text{benzene})_n]^+$ ($m = 1-13$, $n = 1-4$) complexes. In this experiment apparatus, the reactions happened under about 200−270 K in the tube reactor, and the products were cooled to about 150 K by supersonic expansion into the vacuum (simulation results using the 3D-hydro program[24]). In these formed complexes, benzene molecules should be adsorbed on lead cluster cations through chemical interactions.

The distribution of $[Pb_m(\text{benzene})_n]^+$ series had several characteristics. First, the number of adsorbed benzene molecules was less than four for all lead cluster cations ($m = 1-13$); second, except $[Pb(\text{benzene})_n]^+$ and $[Pb_2(\text{benzene})_n]^+$, $[Pb_m(\text{benzene})_n]^+$ had monotonically decreasing intensities as n increased, and no "magic number" peaks were observed; third, the larger the lead clusters were, the fewer of benzene molecules could be adsorbed. All of these characters were independent of the concentration of benzene reagent in argon gas.

This result was consistent with that of the reactions between Pb_m^+ and methanol,[16] for which no apparent "magic number" peaks or abrupt intensity decrease appeared in the product series. This characteristic was very different from that of transition metal species. For example, in the sandwich complexes of Sc, Ti, V, etc., $[M_m(\text{benzene})_{m+1}]$ peaks showed apparently enhanced intensity, while for rice-ball complexes of Fe, Co, Ni, etc., the number of absorbed benzene molecules increased with the increasing size of the metal moiety and was governed by the d−π bonding pattern and the effect of steric hindrance.

Thermochemical study using high-pressure mass spectrometry[15] showed that the properties of reaction $Pb^+ +$ benzene ↔

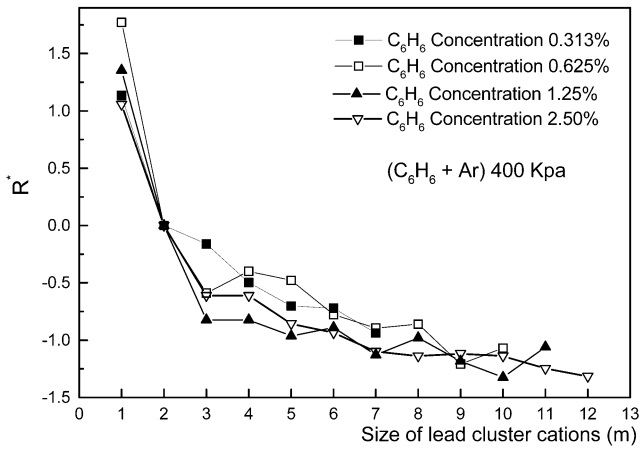

Figure 2. The dependence of R_m* on the size of cationic lead clusters when different benzene concentrations were used (the pressure of the mixed gas was 400 kPa; $R_m^* = \ln\{[I_{m,1}/I_{m,0}]/[I_{2,1}/I_{2,0}]\}$; $I_{m,0}$, $I_{m,1}$, $I_{2,0}$, and $I_{2,1}$ stood for the intensities of Pb_m^+, $[Pb_m(benzene)]^+$, Pb_2^+, $[Pb_m(benzene)]^+$, respectively).

$[Pb(benzene)]^+$ were as follows: $-\Delta H^\circ = 26.2 \pm 0.4$ kcal/mol, $-\Delta S^\circ = 21.6 \pm 0.6$ cal/mol, and the electrostatic interaction dominated the interaction. From the intensity distribution of Pb_m^+ and $[Pb_m(benzene)]^+$, we could deduce some information about the absorption of benzene on different size cationic lead clusters. Because the simple absorption process was defined as one with a negligible barrier and no metastable precursor states and could reach equilibrium easily under high-pressure condition,[25] the adsorption free energy of benzene on different size Pb_m^+ ($Pb_m^+ +$ benzene $\leftrightarrow [Pb_m(benzene)]^+$) could be obtained as follows:

$$\Delta G_m = RT \ln\{I_{m,1}/[I_{m,0}(\text{benzene})]\} \quad (1)$$

$I_{m,0}$ and $I_{m,1}$ stood for the peak intensities of Pb_m^+ and $[Pb_m(benzene)]^+$, respectively, and (benzene) stood for the partial pressure of benzene reagent. To remove the parameters of (benzene) and T (about 200−270 K), the exact values of which were difficult to determine, we defined the R_m* as the relative free energy comparing to ΔG_2:

$$R_m^* = (\Delta G_m - \Delta G_2)/(RT) = \ln\{[I_{m,1}{}^*I_{2,0}]/[I_{m,0}{}^*I_{2,1}]\} \quad (2)$$

As shown in Figure 2, the results of different benzene concentrations showed a good consistency. The R_m* decreased slowly, as well as smoothly, and no obvious turning point existed. In conclusion of the cation product results, we believed that the electrostatic interaction contributed mainly to the absorption. The chemical bonds involving donation−acceptance of valence electrons, such as the cases in transition metal−benzene complexes, could be excluded. The positive charge dispersion on the larger lead moiety weakened the electrostatic interaction and therefore caused the decreasing of R_m*. The formation processes of the above products should occur via eqs 3 and 4. It has been shown that the association products form

$$Pb_m{}^+ + (\text{benzene})_n \leftrightarrow [Pb_m(\text{benzene})_n]^{+*} \xrightarrow{Ar} [Pb_m(\text{benzene})_n]^+ \quad (3)$$

$$[Pb_m(\text{benzene})_n]^+ \leftrightarrow [Pb_m(\text{benzene})_{n1}]^+ - (\text{benzene})_{n2} \quad (4)$$

easily at low collision energies and under multiple-collision condition.[26] They could be stabilized by collisions with the carrier gas or by evaporation of benzene molecules.

SCHEME 1 The Isomer Structures with the Lowest Energy for (A) $[Pb(C_5H_5)]^+$, (B) $[Pb(C_7H_5)]^+$, (C) $[Pb(C_5H_5)(C_6H_6)]^+$, and (D) $[Pb(C_7H_5)(C_6H_6)]^+$

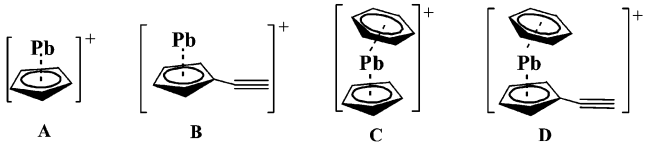

3.1.2. Pb/Benzene Dissociated Cation Products. In the low-mass region, close to the $[Pb(benzene)]^+$, peaks near 273 and 297 Da were observed. Those peaks were assigned as $[Pb(C_5H_5)]^+$ and $[Pb(C_7H_5)]^+$, which originated from the dissociative reactions of benzene on lead cations. As shown in eq 5, the C−C bond in benzene cleaved and the structure rearranged through loss of certain neutral fragments (possibly [CH] or $[C_5H_7]$). Reactions between lead cations and benzene cluster also formed $[Pb(C_5H_5)(C_6H_6)]^+$, $[Pb(C_7H_5)(C_6H_6)]^+$, and $[Pb(C_7H_5)(C_6H_6)_2]^+$ species.

$$Pb^+ + (C_6H_6)_n \rightarrow [Pb(C_5H_5)(C_6H_6)_k]^+ + [CH] + (n-k)C_6H_6 \quad (k = 0, 1)$$

$$\rightarrow [Pb(C_7H_5)(C_6H_6)_k]^+ + [C_5H_7] + (n-k-1)C_6H_6 \quad (k = 0, 1, 2) \quad (5)$$

DFT calculations on $[Pb(C_5H_5)]^+$ and $[Pb(C_7H_5)]^+$ (B3LYP method with 6-31++G** basis sets for C and H atoms and 5s5p5d/4s4p1d basis sets for Pb atom) showed that the most probable isomers were Pb/cyclopentadienyl conjugation structures (Scheme 1), which were the lowest-energy isomers on the potential energy surface (detailed calculation results are going to be reported elsewhere; here only outline is given). For $[Pb(C_5H_5)^+]$ (A in Scheme 1), Pb atom combined with the five C atoms equally, as the result in ref 27. $[Pb(C_7H_5)^+]$ (B in Scheme 1) was also Pb/cyclopentadienyl conjugation structure with a C≡C side chain. Calculation results also revealed that $[Pb(C_5H_5)(C_6H_6)]^+$ and $[Pb(C_7H_5)(C_6H_6)]^+$ species were bent sandwich structures (see Scheme 1, C and D structures). This was reasonable considering that both of them were isoelectronic to the neutral $[M(C_5H_5)_2]$ (M = Si−Pb) molecules, which were typical bent sandwich molecules in gas phase.[28,29]

3.2. Reactions between Lead Cluster Anions and Benzene. In comparison with the cases of cations, the reactions between anionic lead clusters and benzene were tremendously different. Two typical TOF mass spectra of the anionic products were shown in Figures 3 and 4. The concentrations of benzene reagent in argon gas were 0.625% and 0.075%, respectively.

As shown in Figure 3A, when the benzene concentration was 0.625% (the partial pressure of benzene is 2.5 kPa in 400 kPa mixed gas), the dominant products were $[Pb_mC_n]^-$ ($m = 1-6$, $n = 1-16$) and $[Pb_mC_nH_k]^-$ ($m = 1-6$, $n = 1-16$, $k = 1-5$). Figure 3B−E showed the hydrogen resolution results of these products. When $n \leq 3$, $[Pb_mC_n]^-$ clusters could hardly be detected, which indicated that these clusters were difficult to form under the present experimental condition. For a given m value, $[Pb_mC_n]^-$ and $[Pb_mC_nH_k]^-$ had first a monotonically increasing and then monotonically decreasing intensity distribution with the special intensity of ion clusters at $n = 4$, 5, 7, and 8. As we know, the benzene decomposition processes on metal cluster was quite complex, and the underlying mechanism for this decomposition process was presumably determined by the thermodynamics. We decreased the benzene concentration to 0.075% (mixed 0.3 kPa of benzene in the 400 kPa mixed gas),

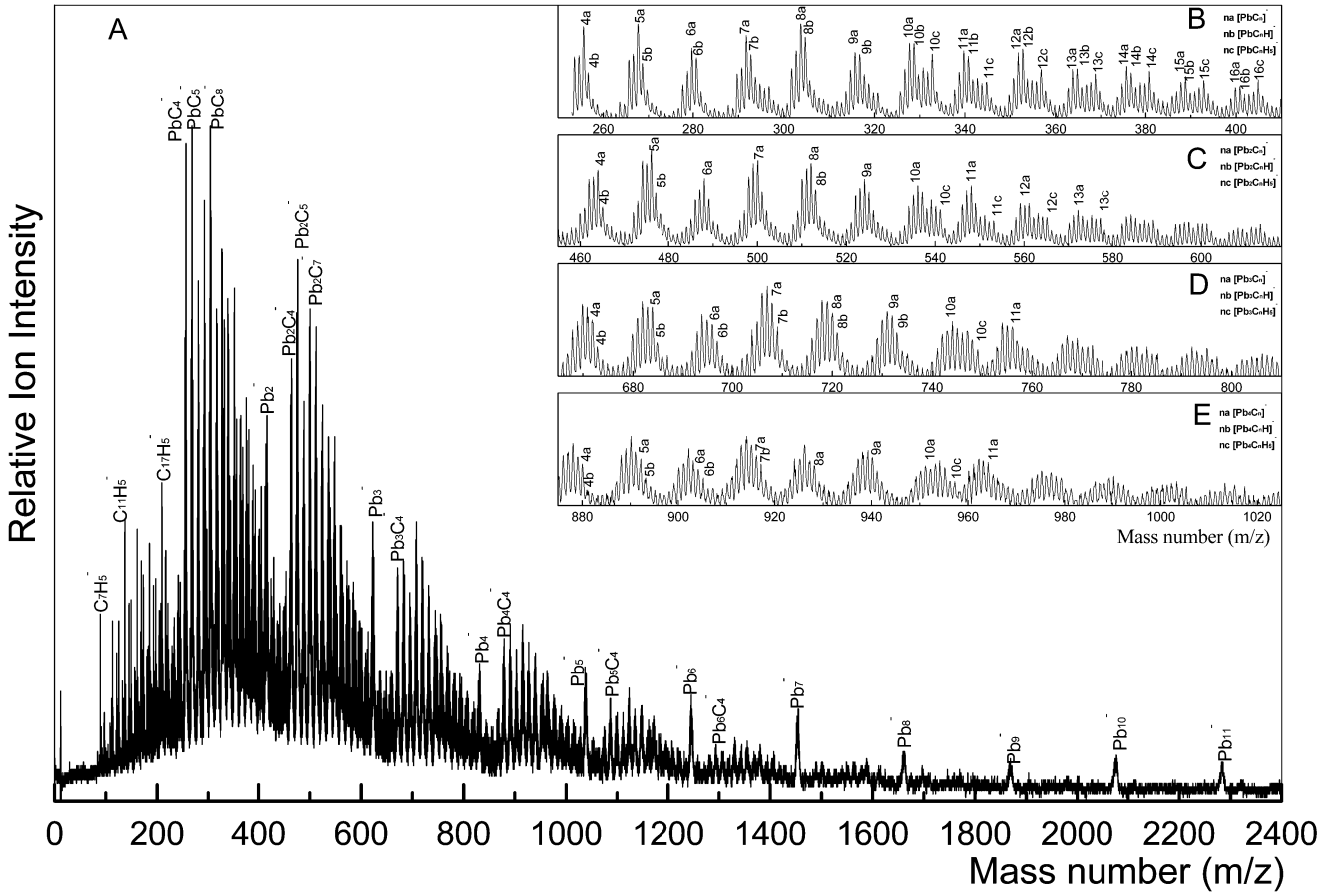

Figure 3. Typical mass spectra of the anion products by laser ablation of lead into a mixture of argon and high concentration of benzene (0.625% benzene in 400 kPa mixed gas). The inserts (panel B from 250 to 410 Da, panel C from 455 to 618 Da, panel D from 665 Da to 810 Da, and panel E from 875 to 1025 Da) were the enlarged mass fields showing the isotope distributions of anion products ($[Pb_mC_n]^-$, $[Pb_m(C_nH_k)]^-$, etc.).

and the typical mass is shown in Figure 4A. Figure 4B−E shows the hydrogen resolution results of the dominant products. They were assigned as $[Pb_m(C_6H_5)]^-$ ($m = 1-7$). $[Pb_mC_n]^-$ ($m = 1-4$, $n = 1-10$) species were also observed even they have low ion intensity, while little anion [Pb/benzene]$^-$ association products were detected.

To determine the relationships between these several product species, the products under different benzene concentrations were analyzed in detail. Figure 5 showed the statistical relative intensities of four representative product series (Pb_m^-, $[Pb_mC_4]^-$, $[Pb_mC_7]^-$, and $[Pb_m(C_6H_5)]^-$) with different benzene concentrations (0.075% (A), 0.15% (B), 0.313% (C) and 0.625% (D) in 400 kPa mixed gas). This picture clearly indicated that $[Pb_m(C_6H_5)]^-$ species were absolutely predominant anion product when the concentration of benzene reagent was low while difficult to detect in the high benzene concentration systems. The intensities of $[Pb_mC_4]^-$ or $[Pb_mC_7]^-$ followed the reverse trend. These results revealed that $[Pb_m(C_6H_5)]^-$ species should be the dominant products produced by the initial reaction step, and the following steps formed $[Pb_mC_n]^-$, $[Pb_mC_nH_k]^-$, etc. series. These processes could be described with eqs 6 and 7. In

$$Pb_m^- + (C_6H_6) \leftrightarrow [Pb_m\cdots(C_6H_5)]^{-*} \xrightarrow{Ar} [Pb_m(C_6H_5)]^- + [H] \quad (6)$$

$$[Pb_m(C_6H_5)]^- + (C_6H_6)_n \rightarrow [Pb_mC_n]^-, [Pb_mC_nH_k]^- \text{ (quenched by argon)} \quad (7)$$

the $[Pb_m(C_6H_5)]^-$ species, the phenyl group should combine on lead clusters through one Pb−C σ bond.

3.3. Reactions between Neutral Lead Clusters and Benzene. The possible neutral products in the reactions between lead clusters and benzene were detected through ionization by another laser (ArF excimer, 193 nm, 0−20 mJ/pulse, 1 mm in diameter of the focused beam spot). Figure 6A was a typical mass spectrum of the blank experiment (no lead cluster were introduced), in which the dominant species were benzene clusters and hydrocarbon fragments ($[CH_{0,1}]$, $[C_2H_{0-4}]$, $[C_3H_{0-4}]$, and $[C_4H_{0-4}]$). Figure 6B was the result when the lead clusters were introduced. Figure 6A,B showed nearly the same species and intensities, except that three new products, $[Pb(C_7H_5)]^+$, Pb^+, and Pb_2^+, appeared in Figure 6B. The hydrocarbon fragments in Figure 6B ($[CH_{0,1}]$, $[C_2H_{0-4}]$, $[C_3H_{0-4}]$, and $[C_4H_{0-4}]$) were similar as those in the blank experiment (come from the dissociation of pure benzene clusters). $[Pb(C_7H_5)]$ species might have similar formation pathway as the cation product $[Pb(C_7H_5)]^+$. Even when we scanned the power of the ArF laser, no association complexes, metal−carbon clusters, metal−phenyl complexes, or carbon clusters were observed. The only reason for this was that the intensities of those species were too low to be detected. So, we suggest that the interaction between neutral lead clusters and benzene mainly formed physisorbed species, which could not survive to be ionized, extracted and detected. Our calculation (based on the same theoretical level with that described in section 3.1) results indicated that the Pb−benzene interaction energy was less than 10 kcal/mol. This process can be described as eq 8.

$$Pb_m + (\text{benzene})_n \leftrightarrow [Pb_m\cdots(\text{benzene})_n] \text{ (physisorbed species)} \quad (8)$$

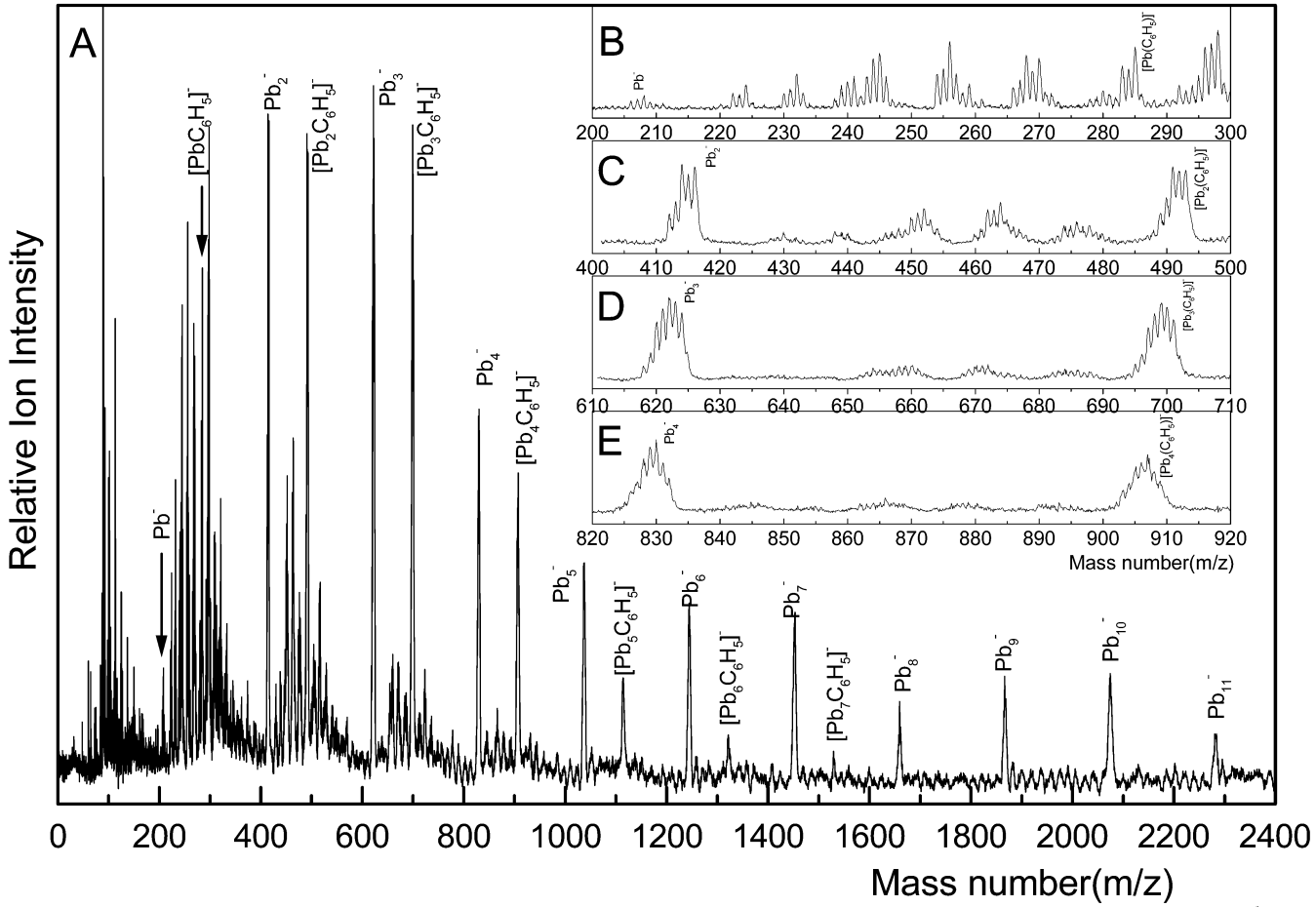

Figure 4. Typical mass spectra of the anion products by laser ablation of lead into a mixture of argon and low concentration of benzene (0.075% benzene in 400 kPa mixed gas). The inserts (panel B from 200 to 300 Da, panel C from 400 to 500 Da, panel D from 610 to 710 Da, and panel E from 820 to 920 Da) were the enlarged mass fields showing the isotope distributions of anion products (Pb_m^+, $[Pb_m(C_6H_5)]^+$, etc.).

3.4. Summarized Reaction Mechanisms. Under the present condition, argon acted as buffer and also cooling gas, where benzene reagents were seeded directly. The lead particles produced by laser ablation grew larger, interacted with benzene, and were cooled by buffer gas in the tube reactor. Because no corresponding neutral products were observed in the experiment, the interaction of anion and cation species could be neglected. This was due to the less possibility because the amount of ions was very small compared with that of benzene molecules or neutral lead particles. We could see that the cation and anion reactions follow two conspicuously different and independent reaction pathways. The summarized reaction mechanisms between lead clusters and benzene were shown in the Scheme 2.

3.4.1. Charge Effects on the Reactions. Association complexes were the dominant products in the reactions between Pb_m^+ and benzene. When $m > 1$, even when the benzene concentration was up to 2.5% (partial pressure of benzene was up to 10 kPa in the argon gas), no apparent dissociated products were detected. This showed that lead cluster cations could hardly dissociate benzene molecules in gas phase. As discussed in sections 3.1.1 and 3.3, benzene could not form donor−acceptor bonds on lead cluster surface, and the adsorption was mainly electrostatic interaction. As for the $[Pb(C_5H_5)]^+$, $[Pb(C_7H_5)]^+$ etc., the detailed reaction process could not be traced yet. In our previous studies,[17] $[Pb(C_5H_5)]^+$ was also observed from the reaction between lead cluster cations with butene. The formation pathway surely involved C−C break and fragment rearrangement on Pb^+.

The negative charges on metal surfaces could weaken the metal−benzene interaction, as pointed out in ref 30. It was for this that no lead cluster−benzene anions were observed. When lead cluster anions interacted with benzene molecules, the excess energy within the clusters or originating from the collisions could ignite the dehydrogenating reactions, in which the $[Pb_m(C_6H_5)]^-$ series were most important intermediates. Because the following decomposition process and carbide formation were exothermic, the energy released could usually promote the dissociation and "evaporation" of hydrogen from the small molecules.[30−32] However when the low concentration benzene reagent was used, the reactions could be easily quenched by cooling gas and stopped at $[Pb_m(C_6H_5)]^-$ species. The dependence of the dominant products on the concentration of benzene shown in Figure 5 also implied that the formation of $[Pb_m(C_6H_5)]^-$ should be the initial step of the reactions.

For the usual dehydrogenation of benzene on metal surface,[30−32] the H atoms were eliminated as H_2 molecule, because this pathway was thermodynamically preferred. However, under certain conditions, the selective C−H cleavage of benzene could be achieved. For example, electron (5−10 eV)−benzene interaction could produce $C_6H_5^-$ and H in gas phase.[33] This involved one repulsive state of benzene, and C−H cleavage is dynamically favored. Electron-induced dissociation (typically 10−50 eV) of benzene on Ag or Au surface can also produce clean absorbed phenyl group.[34−36] In these reactions, the proposed mechanism involved an electron impact ionization process, and the quick C−H cleavage of the intermediate $C_6H_5^+$ was dynamically favored. In our experiment, one new pathway

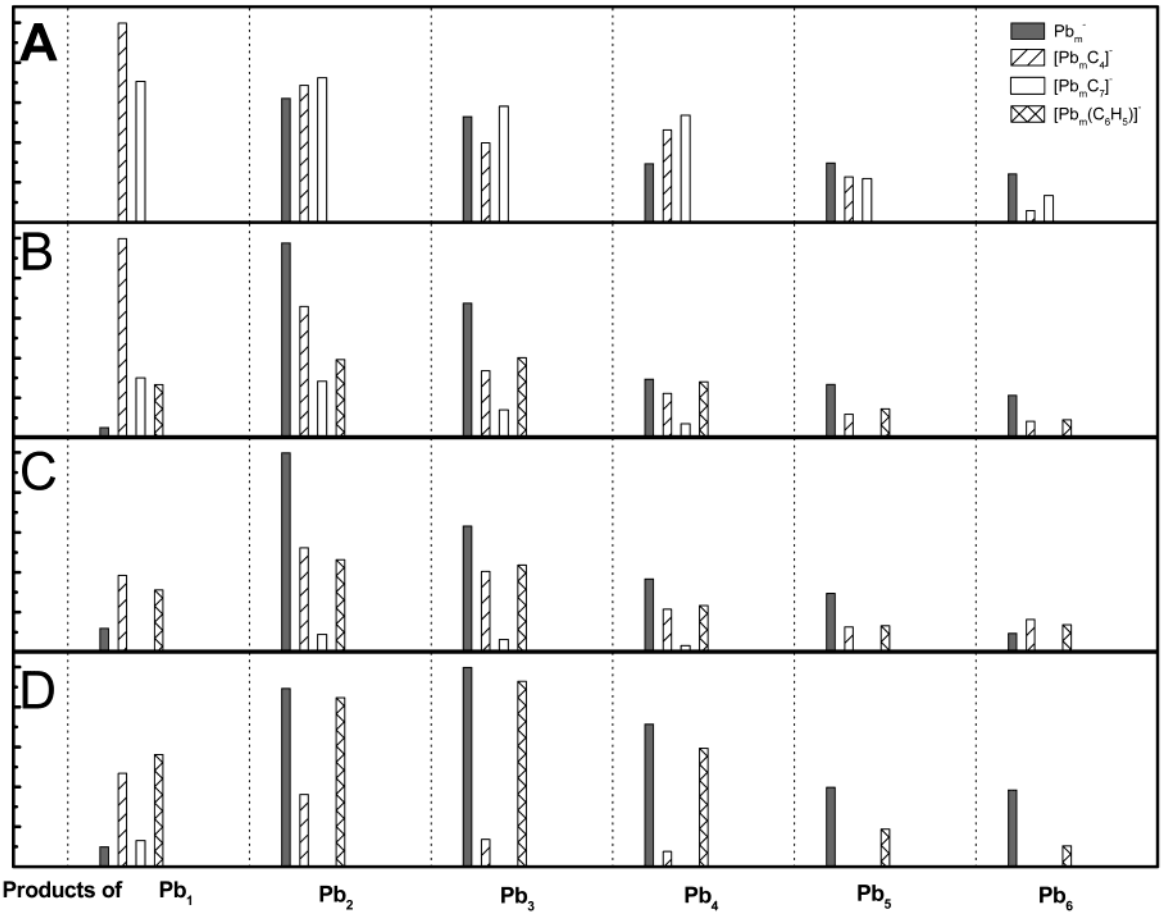

Figure 5. The statistical relative intensities of four representative product series (Pb_m^-, $[Pb_mC_4]^-$, $[Pb_mC_7]^-$, and $[Pb_m(C_6H_5)]^-$ when different concentrations of benzene (panel A, 0.625%; panel B, 0.313%; panel C, 0.15%; panel D, 0.075%) in total 400 kPa mixed gas were used.

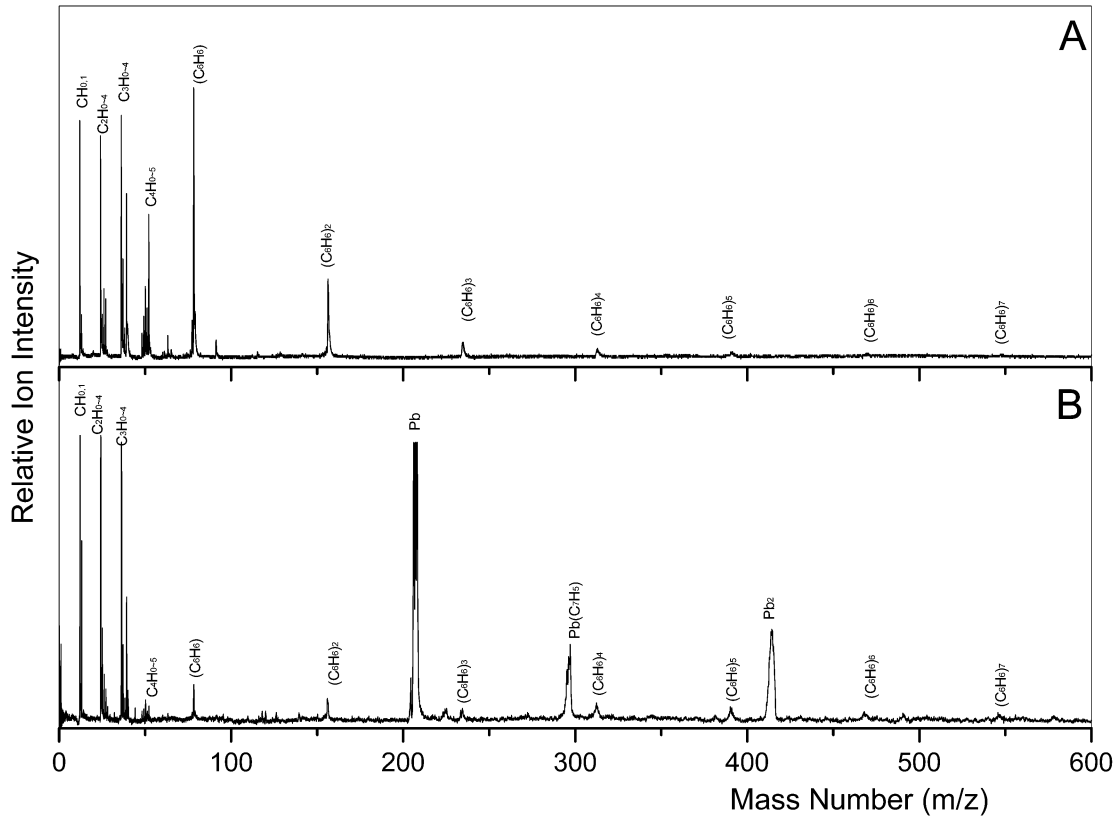

Figure 6. The typical mass spectrum (A) of the cations produced by ionization of benzene and (B) of the cations produced by ionization of the neutral products in the reactions between lead clusters and benzene (1.25% benzene in 400 kPa mixed gas, 193 nm ArF laser, 10 mJ/pulse, and 1 mm in diameter of the focused beam spot).

SCHEME 2: Proposed Reaction Mechanisms between Lead Clusters (Cations, Anions, and Neutral) and Benzene in Gas Phase

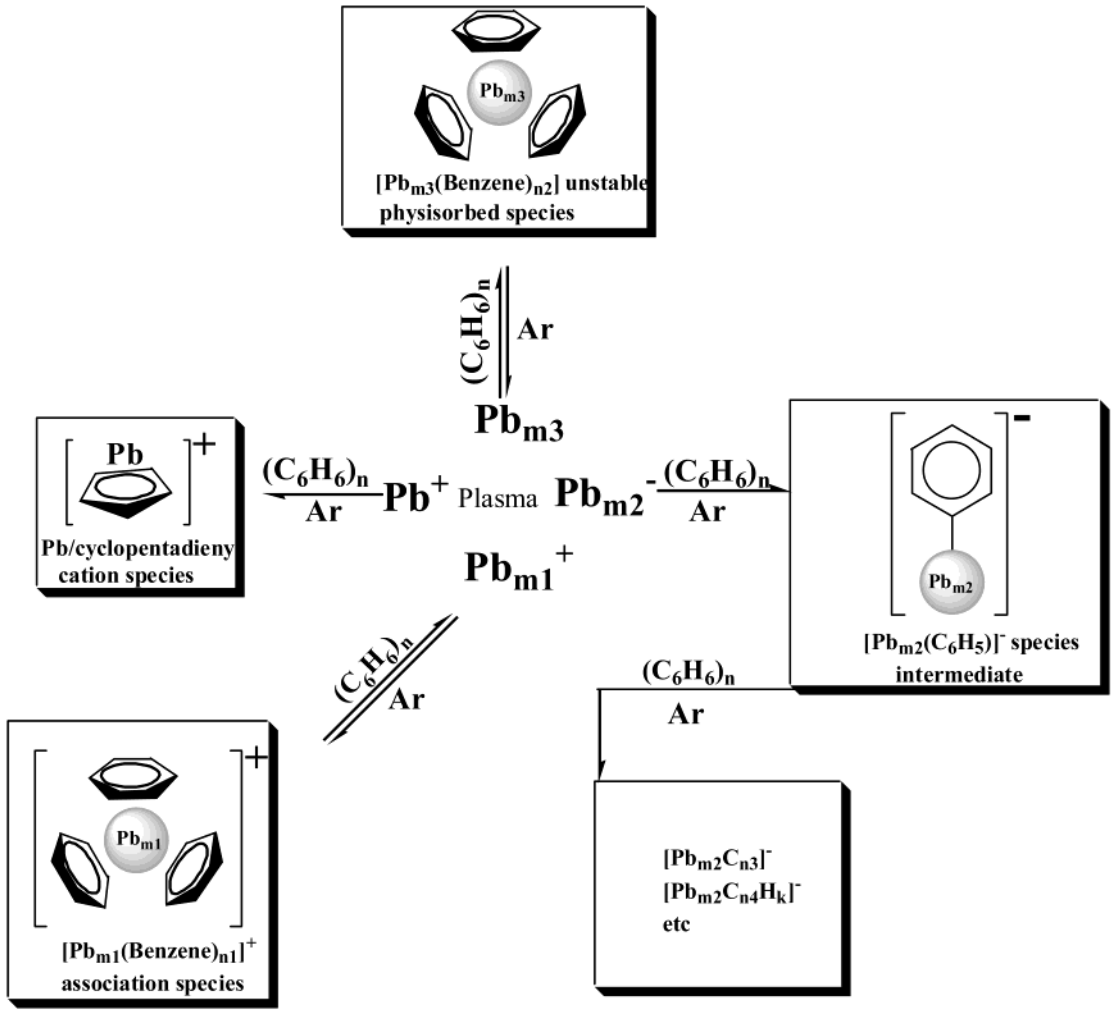

was found to achieve the selective C−H cleavage of benzene in gas phase. The negative charge on lead cluster anions could be partially transferred to the benzene molecule, and the excessive energy originating from the hot cluster anions or the collision with benzene would induce the C−H break. Because the possible formed $[Pb_m\cdots(C_6H_5)]^-$* in eq 6 could be quenched quickly through dissociation to lead cluster anions again, the quick C−H cleavage process should be dynamically favored compared with other slow processes such as H_2 evaporation or C−C break.

3.4.2. Size Effects on the Reactions. The size effects have been observed in the reactions of cations or anions. In the cation cases, the R_m* decreased apparently with the increasing of m. In the anion cases, the reactions happened mainly on those clusters for which $m \leq 7$. These were due to the following reasons: first, with the increasing cluster size, the positive or negative charge became dispersed, and the reactions were restrained; second, lead clusters ($m > 4$) tended to assume compact near-spherical structure,[37] and with the increasing size, the effects of edges or end atoms would decrease. As result, the smaller lead cluster ions were always more reactive.

4. Conclusion

On a high-resolution reflectron time-of-flight mass spectrometer (RTOFMS) with a laser ablation argon buffer gas ion source, the reactivity of lead cluster ions with benzene was studied. Conspicuously different reactions were observed for cations and anions. The main results were summarized as follows. (1) The Pb_m^+ ($m > 1$) clusters could only adsorb 1−4 benzene molecules, and no dissociated products were observed. In the formed $[Pb_m(\text{benzene})_n]^+$ complexes, the electrostatic interaction contributed mainly to the adsorption. Pb^+ could dissociate benzene molecules or clusters, forming $[Pb(C_5H_5)\text{-}(C_6H_6)_n]^+$ ($n = 0, 1$) or $[Pb(C_7H_5)(C_6H_6)_n]^+$ ($n = 0, 1, 2$). The DFT calculations showed that they contained Pb/cyclopentadienyl structure. (2) The Pb_m^- clusters could promote the "evaporation" of hydrogen and carbon atoms from benzene molecules, forming $[Pb_mC_n]^-$ and $[Pb_mC_nH_k]^-$ products, and the initial step of the reactions was to break only one C−H bond, forming $[Pb_m(C_6H_5)]^-$ complexes. (3) The interactions between neutral lead clusters and benzene mainly formed physisorbed species, which could not survive to be detected under our experimental condition. (4) The reactions of lead cluster cations and anions followed two conspicuously different and independent reaction pathways. The reaction mechanism showed clearly the charge effects on the reactions. Additionally the size effects of lead clusters (cations, as well as anions) were also observed, and the smaller sized clusters were always more reactive.

5. Commentary

On the basis of the above results, we believed that on the solid metal surfaces (for example, many catalysis surfaces) the

microsurroundings involving charges should play an important role in the reactions of hydrocarbon molecules such as benzene and negative charges tend to activate these molecules, as have been observed in gas phase. Additionally, the metal cluster−phenyl complexes observed in this experiment were very rare cases in organometallic chemistry, while they are very important intermediate species in many homogeneous catalysis processes (as mentioned in refs 34−36). The anion lead−phenyl complexes observed in this experiment present an opportunity to study their bond patterns and electron states in detail in gas phase. This work is currently in progress.

Acknowledgment. The authors gratefully acknowledge the support of the National Natural Science Foundation of China under Grant 20203020. We are indebted to Professor Qihe Zhu and Zhen Gao for their original design and assembly of the experimental apparatus. We are also indebted to Professor Hongfei Wang and Fanao Kong for their helpful discussions. We thank Dr. Haisheng Chen (Institute of Engineering Thermophysics, CAS) for helping us to simulate the reaction temperature in our instrument.

References and Notes

(1) Mulliken, R. S. *J. Am. Chem. Soc.* **1952**, *64*, 811.
(2) Haaland, A. *Acta Chem. Scand.* **1965**, *19*, 41.
(3) Jacobson, D. B.; Freiser, B. S. *J. Am. Chem. Soc.* **1984**, *106*, 3900.
(4) Trevor, D. J.; Whetten, R. L.; Cox, D. M.; Kaldor, A. *J. Am. Chem. Soc.* **1985**, *107*, 518.
(5) Meyer, F.; Khan, F. A.; Armentrout, P. B. *J. Am. Chem. Soc.* **1995**, *117*, 9740.
(6) Ma, J. C.; Dlugherty, D. A. *Chem. Rev.* **1997**, *97*, 1303.
(7) Willey, K. F.; Cheng, P. Y.; Bishop, M. B.; Duncan, M. A. *J. Am. Chem. Soc.* **1991**, *113*, 4721.
(8) Willey, K. F.; Yeh, C. S.; Robbins, D. L.; Duncan, M. A. *J. Phys. Chem.* **1992**, *96*, 9106.
(9) Hosshino, K.; Kurikawa, T.; Takeda, H.; Nakajima, A.; Kaya, K. *J. Phys. Chem.* **1995**, *99*, 3035.
(10) Kurikawa, T.; Hirano, M.; Takeda, H.; Yagi K.; Hoshino, K.; Nakajima, A.; Kaya, K. *J. Phys. Chem.* **1995**, *99*, 16429.
(11) Kurkawa, T.; Takeda, H.; Hiranok, M.; Judai, K.; Arita, T.; Nagao, S.; Nakajima, A.; Kaya, K. *Organometallics* **1999**, *18*, 1430.
(12) Venkatachalapathy, R.; Davila, G. P.; Prakash, J. *Electrochem. Commun.* **1999**, *1*, 614.
(13) Halligudi, S. B.; Kala Raj, N. K.; Rajani, R.; Unni, I. R.; Gopinathan, S. *Appl. Catal., A* **2000**, *204*, L1.
(14) Tang, I. N.; Castleman, A. W. *J. Chem. Phys.* **1972**, *57*, 3638.
(15) Guo, B. C.; Purnell, J. W.; Castleman, A. W., Jr. *Chem. Phys. Lett.* **1990**, *168*, 155.
(16) Barran, P. E.; Mikhailov, V.; Stace, A. J. *J. Phys. Chem. A* **1999**, *103*, 8792.
(17) Tian, Z. X.; Xing, X. P.; Tang, Z. C. *Rapid Commun. Mass Spectrom.* **2002**, *16*, 1515.
(18) Tian, Z. X.; Xing, X. P.; Tang, Z. C. *Rapid Commun. Mass Spectrom.* **2003**, *17*, 17.
(19) Maruyama, S.; Anderson, L. R.; Smalley, R. E. *Rev. Sci. Instrum.* **1990**, *61*, 3686.
(20) Mamyrin, B. A.; Shmikk, D. V. *Sov. Phys. JETP* **1979**, *49*, 762.
(21) Xing, X. P.; Tian, Z. X.; Liu, P.; Gao, Z.; Zhu, Q. H.; Tang, Z. C. *Chin. J. Chem. Phys.* **2002**, *15*, 83.
(22) Lu, W.; Huang, R. B.; Yang, S. H. *J. Phys. Chem.* **1995**, *99*, 12099.
(23) Phillips, J. C. *J. Chem. Phys.* **1987**, *87*, 1712.
(24) Hirsch, C.; Lacor, C.; Dener, C.; Vucinic, D. *AGARD-CP-510*; NATO: Brussels, Belgium, 1992.
(25) William, T. W.; Robert, L. W. *J. Phys. Chem. B* **2000**, *104*, 10964.
(26) Clemmer, D. E.; Chen, Y. M.; Khan F. A.; Armentrout P. B. *J. Phys. Chem.* **1994**, *98*, 6522.
(27) Almenningen A.; Haland A.; Motzfeldt T. *J. Organomet. Chem.* **1967**, *7*, 97.
(28) Smith, J. D.; Hanusa, T. P. *Organometallics* **2001**, *20*, 3056.
(29) Armstrong, D. R.; Duer, M. J.; Dacidson, M. G.; Moncrieff, D.; Russell, C. A.; Stourton, C.; Steiner, A.; Stalke, D.; Wright, D. S. *Organometallics* **1997**, *16*, 3340.
(30) Berg, C.; Beyer, M.; Achatz, U.; Joos, S.; Niedner-Schatteburg, G.; Bondybey, V. E. *J. Chem. Phys.* **1998**, *108*, 5398.
(31) Berg, C.; Schindler, T.; Kantlehner, M.; Schatterburg, G. N.; Bondybey, V. *Chem. Phys.* **2000**, *262*, 143.
(32) Albert, G.; Berg, C.; Beyer, M.; Achatg U.; Jods, S. *Chem. Phys. Lett.* **1997**, *268*, 235.
(33) Dillard, J. G. *Chem. Rev.* **1973**, *73*, 589.
(34) Zhou, X.-L.; Castro, M. E.; White, J. M. *Surf. Sci.* **1990**, *238*, 215.
(35) White, J. M. *Langmuir* **1994**, *10*, 3946.
(36) Syomin, D.; Kim, J.; Koel, B. E. *J. Phys. Chem. B* **2001**, *105*, 8387.
(37) Shvartsburg, A. A.; Jarrold, M. F. *Chem. Phys. Lett.* **2000**, *317*, 615.